Available online at www.sciencedirect.com
SCIENCE DIRECT®
International Journal of Heat and Mass Transfer 49 (2006) 658–670
International Journal of HEAT and MASS TRANSFER
www.elsevier.com/locate/ijhmt

Evaporation heat transfer and pressure drop of HFC-134a in a helically coiled concentric tube-in-tube heat exchanger

Somchai Wongwises *, Maitree Polsongkram

Fluid Mechanics, Thermal Engineering and Multiphase Flow Research Laboratory (FUTURE), Department of Mechanical Engineering, King Mongkut's University of Technology Thonburi, Bangmod, Bangkok 10140, Thailand

Received 1 June 2005; received in revised form 18 August 2005
Available online 18 October 2005

Abstract

The two-phase heat transfer coefficient and pressure drop of HFC-134a during evaporation inside a smooth helically coiled concentric tube-in-tube heat exchanger are experimentally investigated. The test section is a 5.786-m long helically coiled tube with refrigerant flowing in the inner tube and heating water flowing in the annulus. The inner tube is made from copper tubing of 9.52 mm outer diameter and 7.2 mm inner diameter. The heat exchanger is fabricated by bending a straight copper tube into a spiral coil. The diameter of coil is 305 mm. The test run are done at average saturated evaporating temperatures ranging between 10 and 20 °C. The mass fluxes are between 400 and 800 kg m^{-2} s^{-1} and the heat fluxes are between 5 and 10 kW m^{-2}. The inlet quality of the refrigerant in the test section is calculated using the temperature and pressure obtained from the experiment. The pressure drop across the test section is directly measured by a differential pressure transducer. The effects of heat flux, mass flux and, evaporation temperature on the heat transfer coefficients and pressure drop are also discussed. The results from the present experiment are compared with those obtained from the straight tube reported in the literature. New correlations for the convection heat transfer coefficient and pressure drop are proposed for practical applications.

Keywords: Two-phase; Evaporation; Heat transfer coefficient; Pressure drop; Refrigerant; Helically coiled tube

1. Introduction

Results from many researches show that the ozone layer is being depleted. The general consensus for the cause of this event is that the free chlorine radicals removes ozone from the atmosphere and later the chlorine atom is continued to convert more ozone to oxygen. The presence of chlorine in the stratosphere is the result of migration of chlorine-containing chemicals. The chlorofluorocarbons (CFCs) is a large class of chemicals which behaves in this manner. These chemicals have many unusual properties for example, nonflammability, low toxicity, and material compatibility that have led to their common widespread use, both consumers and industries around the world as refrigerants, solvent, and blowing agents for foams. Since the depletion of the earth's ozone layer has been discovered, many corporations have been forced to find alternative chemicals to CFCs. Because the thermophysical properties of HFC-134a are very similar to those of CFC-12. Refrigerant HFC-134a is receiving the supporting from the refrigerant and air-conditioning industry as a potential replacement for CFC-12. However, even the difference in properties between both refrigerants is small but it may result in significant differences in the overall system performance. Therefore, the properties of HFC-134a should be studied in detail before it is applied.

Heat transfer and pressure drop characteristics of refrigerants have been studied by a large number of researchers, both experimentally and analytically, mostly in a horizontal straight tube. The study of the heat transfer and pressure drop inside helicoidal tube has received comparatively little attention in the literature.

* Corresponding author. Tel.: +662 470 9115; fax: +662 470 9111.
E-mail address: somchai.won@kmutt.ac.th (S. Wongwises).

0017-9310/$ - see front matter © 2005 Elsevier Ltd. All rights reserved.
doi:10.1016/j.ijheatmasstransfer.2005.08.017

Nomenclature

A	surface area [m^2]
d_i	inside diameter of inner tube [m]
d_o	outside diameter of inner tube [m]
C_p	specific heat at constant pressure [$J\ kg^{-1}\ K^{-1}$]
D_c	diameter of spiral-coil [m]
G	mass flux [$kg\ m^{-2}\ s^{-1}$]
h	heat transfer coefficient [$kW\ m^{-2}\ K^{-1}$]
i	enthalpy [$kJ\ kg^{-1}$]
k	thermal conductivity [$W\ K^{-1}\ m^{-1}$]
L	total length of helicoidal pipe [m]
m	mass flow rate [$kg\ s^{-1}$]
P	pressure [Pa]
Q	heat transfer rate [kW]
q	heat flux [$kW\ m^{-2}$]
T	temperature [°C]
U	superficial velocity [$m\ s^{-1}$]
x	vapor quality
X_{tt}	Martinelli parameter
z	direction or length [m]

Greek symbols

α	void fraction [–]
μ	dynamic viscosity [Pa s]
ρ	density [$kg\ m^{-3}$]

Dimensionless term

Bo	boiling number
De	Dean number
Nu	Nusselt number
Pr	Prandtl number
Re	Reynolds number

Subscripts

Eq	equivalent
F	frictional term
in	inlet
lv	vaporization latent quantity
out	outlet
ph	pre-heater
ref	refrigerant
sat	saturation condition
tp	two-phase,
TS	test section
l, v	liquid, vapor
w	water
wall	inner tube wall surface contacting the refrigerant

Garimella et al. [1] studied the forced convection heat transfer in coiled annular ducts. Two different coil diameters and two annulars radius ratios were used in the experiment. Hot and cold waters were used as working fluids. They found that the heat transfer coefficients obtained from the coiled annular ducts were higher than those obtained from a straight annulus, especially in the laminar region.

Xin et al. [2] investigated the single-phase and two-phase air–water flow pressure drop in annular helicoidal pipes with horizontal and vertical orientations. Experiments were performed for the superficial water Reynolds number from 210 to 23,000 and superficial air Reynolds number from 30 to 30,000. A friction factor correlation for single-phase flow in laminar, transition and turbulent flow regime was proposed. The two-phase flow pressure drop multipliers in annular helicoidal pipe was found to be dependent on the Lockhart–Martinelli parameter and the flow rate of air or water. The effect of flow rate tended to decrease as the pipe diameter decreased.

Kang et al. [3] studied the condensation heat transfer and pressure drop characteristics of refrigerant HFC-134a flowing in a 12.7 mm helicoidal tube. Experiments were performed for the refrigerant mass flow rate ranging between 100 and 400 $kg\ m^{-2}$, the Reynolds number of the cooling water ranging between 1500 and 9000 at a fixed system temperature of 33 °C, and the temperature of the cooling tube wall ranging between 12 and 22 °C. The effects of cooling wall temperature on the heat transfer coefficients and pressure drops were investigated. The results showed that the refrigerant side heat transfer coefficients decreased with increasing mass flux or the cooling water flow Reynolds number. Correlations obtained from their measured data were proposed and compared with the horizontal straight pipe data.

Rennie and Raghavan [4] used the software package PHEONICS 3.3 to simulate the heat transfer and flow characteristics in a two-turn double tube helical heat exchanger. Simulation in laminar flow region were done for two tube-to-tube ratios, four inner Dean numbers and four annulus Dean numbers. The experimental results showed that at high tube-to-tube ratios, the overall heat transfer coefficient was limited by the flow in the inner tube. Increase of the Dean number, whether in the tube or in the annulus, resulted in the increase of overall heat transfer coefficient.

Yu et al. [5] presented an experimental study on the condensation heat transfer of HFC-134a flowing inside a helical pipe with cooling water flowing in annulus. The experiments were performed for mass flux in the range of 100–400 $kg\ m^{-2}\ s^{-1}$ and the Reynolds number of cooling water in the range of 1500–10,000. They found that the orientations of the helical pipe had significant effects on the heat transfer coefficient.

Louw and Meyer [6] studied the effect of annular contact on the heat transfer coefficients and pressure drop in a helically coiled tube-in-tube heat exchanger. Hot water flowed

in the inner tube, while cold water flowed in the annulus. The heat transfer and pressure drop characteristics of the coiled tube with annular contact were compared with those without annular contact. It was found that annular contact had an insignificant effect on the conduction heat transfer resistance. It made the heat transfer coefficient and pressure drop increase substantially.

It can be noted that the experimental investigations found in the literature described above focused on the study of the condensation heat transfer in a tube-in-tube helical heat exchanger, the study of the evaporation in this kind of heat exchanger remain unstudied. In the present study, the main concern is to obtain and analyze the experimental results of the heat transfer coefficient and pressure drop of the HFC-134a during evaporation in a helically coiled concentric tube-in-tube heat exchanger. The data obtained from the present study are also compared with those obtained from the straight tube reported in the literature. In addition, the large amount of collected data is correlated and used to predict the heat transfer coefficient and pressure drop of the HFC-134a.

2. Experimental apparatus and method

A schematic diagram of the test apparatus is shown in Fig. 1. The test loop consists of a test section, refrigerant loop, heating water flow loops, subcooling loop and the relevant instrumentation. As shown in Fig. 1, the objective of the water loop before entering the test section is to provide controlled inlet quality. The second water loop located in the test section can provide controlled heat input to the test section. The subcooling loop is used to prevent any two-phase flow condition of the refrigerant before entering the refrigerant pump.

For the refrigerant circulating loop, as seen in Fig. 1, liquid refrigerant is discharged by a gear pump which can be regulated by an inverter. The refrigerant then pass in series through a filter/dryer, a sight glass, a refrigerant flow meter, pre-heater, sight glass tube, and entering the test section. The inlet quality before entering the test section is controlled by the pre-heater. Note that the pre-heater is a double-pipe heat exchanger with refrigerant flows inside the tube while water flows in the annulus. Leaving the test section, the refrigerant vapor then condenses in a subcooler and later collected in a receiver and eventually returns to the refrigerant pump to complete the cycle. Instrumentations are located at various positions as clearly seen in Fig. 1 to keep track the refrigerant state. All the signals from the thermocouples and pressure transducer are recorded by a data logger.

The test section is a 5.786-m long helically coiled concentric tube-in-tube heat exchanger with refrigerant flowing in the inner tube and heating water counter currently flowing in the annulus. The inner tube is made from copper tubing of 9.52 mm outer diameter and 7.2 mm inner diameter. The heat exchanger is fabricated by bending a straight

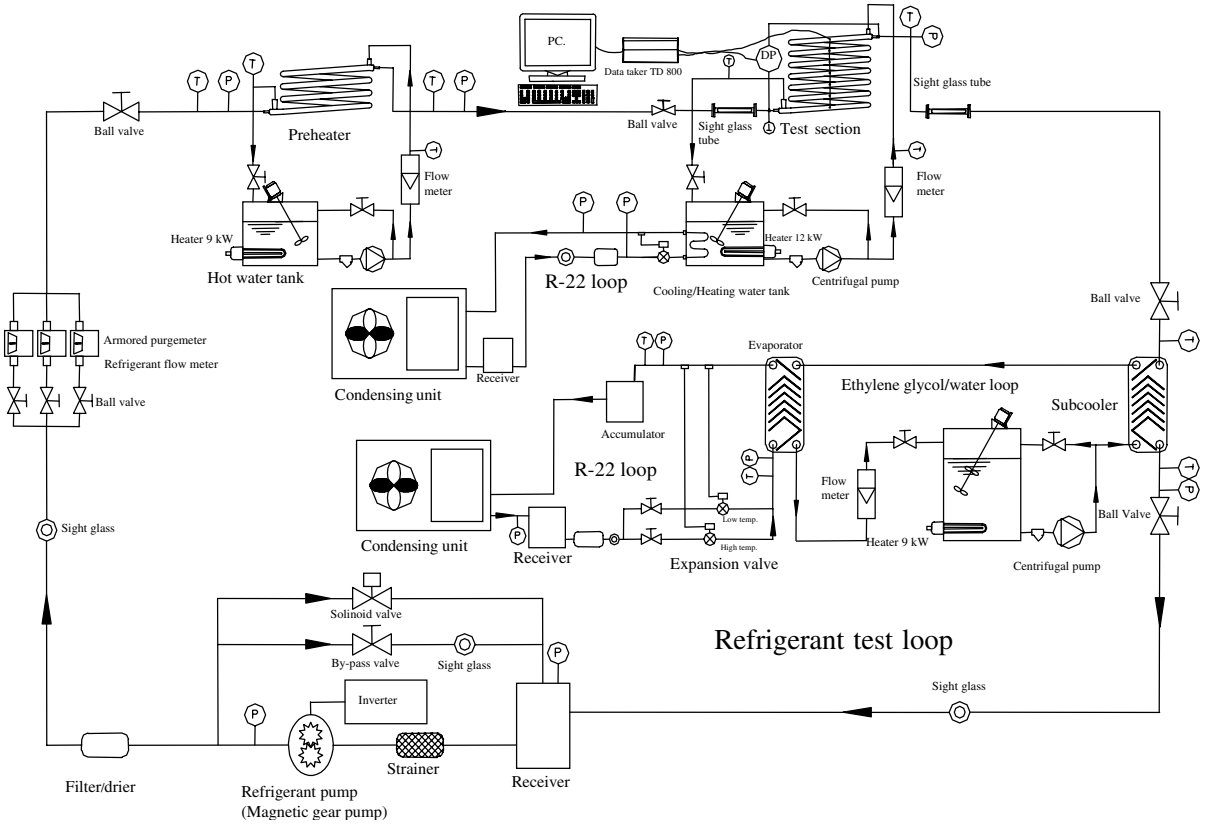

Fig. 1. Schematic diagram of experimental apparatus.

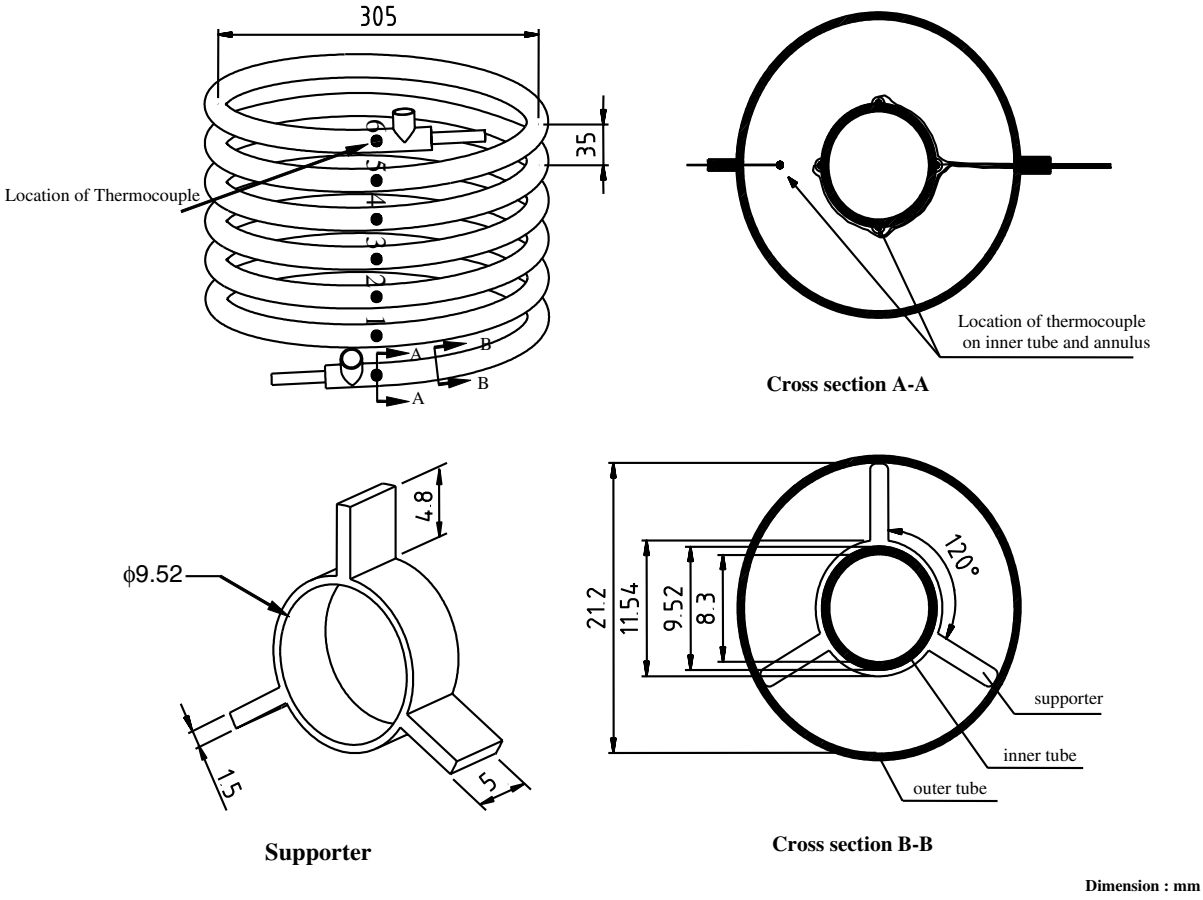

Fig. 2. Schematic diagram of the heat exchanger.

copper into a spiral coil. The diameter of the coil is 305 mm. The helix angle of the coil is 2.09°. Detailed dimension of the heat exchanger is shown in Fig. 2. The dimensions of the test section are also listed in Table 1. The inlet temperature of the water is controlled by a thermostat. A differential pressure transducer and thermocouples are installed in the test section to measure the pressure drop and temperatures across the test section. Detailed dimension of the location of the thermocouples can be seen from Fig. 2.

The refrigerant temperature and tube wall temperatures in the test section are measured by type-T thermocouples. A total of 28 thermocouples are soldered at the top, bottom, and side at seven points along the coiled tube (see Fig. 2). The thermocouples are soldered into a small hole drilled 0.5 mm deep into the tube wall surface and fixed with special glue applied to the outside surface of the copper tubing. With this method, the thermocouples are not biased by the hot water. All the temperature-measuring devices are well calibrated in a controlled temperature bath using standard precision mercury glass thermometers. All static pressure taps are mounted in the tube wall. The refrigerant flow meter is a variable area type. The flow meter is specially calibrated in the range of 0–2.2 gal/min for HFC-134a from the manufacturer. The differential pressure transducers and pressure gauges are calibrated against a primary standard, the dead weight tester. Tests are performed in the steady state. The range of experimental conditions tested in this study is listed in Table 2. The

Table 1
Dimension of the heat exchanger

Parameter	Inner tube	Outer tube
Outside diameter, d_o, mm	9.52	23.2
Inside diameter, d_i, mm	8.3	21.2
Diameter of coil, D_c, mm	305	305
Pitch of coil, p, mm	35	35
Number of turns	6	6
Straight length of the helicoildal pipe, L, mm	5786.8	5786.8

Table 2
Experimental conditions

Mass flux (kg m^{-2} s^{-1})	Temperature (°C)	Heat flux (kW m^{-2})
400	10	5
400	15	5, 10
400	20	5, 10
600	10	5
600	15	5, 10
600	20	5, 10
800	15	5, 10
800	20	5

Table 3
Uncertainties of measured quantities and calculated parameters

Parameter	Uncertainty
Temperature, T (°C)	±0.1 °C
Pressure drop, ΔP (kPa)	±0.075 kPa
Mass flow rate of refrigerant, m_{ref}	±0.1% Full scale
Mass flow rate of water, m_w	±2% Full scale
Mass flux of refrigerant, G	±0.1%
Heat transfer rate of test section, Q_{TS}	±11.39%
Heat transfer rate of pre-heater, Q_{ph}	±9.56%
Boiling heat transfer coefficient, h_{TP}	±12.69%

uncertainties of measured quantities and calculated parameters are shown in Table 3.

3. Data reduction

The following calculation is employed to determine the quality of the refrigerant entering and exiting the test section, and the heat transfer coefficient, from the data recorded during each test run at steady state conditions. The thermodynamic and transport properties of refrigerant are evaluated by using the REFPROP computer program, Version 6.01 [7].

3.1. The inlet vapor quality of the test section ($x_{TS,in}$)

$$x_{TS,in} = \frac{i_{TS,in} - i_{l@T_{TS,in}}}{i_{lv@T_{TS,in}}} \quad (1)$$

where $i_{TS,in}$ is the refrigerant enthalpy at the test section inlet, i_l is the enthalpy of saturated liquid based on the temperature of the test section inlet, and i_{lv} is the enthalpy of vaporization based on the temperature of the test section inlet, and is given by

$$i_{TS,in} = i_{ph,in} + \frac{Q_{ph}}{m_{ref}} \quad (2)$$

where $i_{ph,in}$ is the inlet enthalpy of the liquid refrigerant before entering the pre-heater, m_{ref} is the mass flow rate of the refrigerant, Q_{ph} is the heat transfer rate from the hot water to the refrigerant in the pre-heater

$$Q_{ph} = m_{w,ph} c_{p,w} (T_{w,in} - T_{w,out})_{ph} \quad (3)$$

3.2. The outlet vapor quality of the test section ($x_{TS,out}$)

$$x_{TS,out} = \frac{i_{TS,out} - i_{l@T_{TS,out}}}{i_{lv@T_{TS,out}}} \quad (4)$$

where $i_{TS,out}$ is the refrigerant enthalpy at the test section outlet, i_l is the enthalpy of saturated liquid based on the temperature of the test section outlet, and i_{lv} is the enthalpy of vaporization. As a consequence, the outlet enthalpy of the refrigerant flow is calculated from

$$i_{TS,out} = i_{TS,in} + \frac{Q_{TS}}{m_{ref}} \quad (5)$$

where the heat transfer rate from the hot water to the refrigerant in the test section, Q_{TS}, is obtained from

$$Q_{TS} = m_{w,TS} c_{p,w} (T_{w,in} - T_{w,out})_{TS} \quad (6)$$

3.3. The average heat transfer coefficient

$$h_{tp} = \frac{Q_{TS}}{A_{inside}(\overline{T}_{wall} - \overline{T}_{sat})} \quad (7)$$

where $\overline{T}_{wall}$ is the average temperature of wall and $\overline{T}_{sat}$ is the average temperature of the refrigerant at the test section inlet and outlet. A_{inside} is the inside surface area of the test section;

$$A_{inside} = \pi d_i L \quad (8)$$

where d_i is the inside diameter of the inner tube and L is the length of the test section.

4. Results and discussion

4.1. Average heat transfer coefficient

4.1.1. Effect of mass flux on average heat transfer coefficient

Figs. 3 and 4 show the variations of the average heat transfer coefficient versus average quality during evaporation at constant saturation temperature and heat flux, and at various mass flux values. It was found that the heat transfer coefficient increased with increasing vapour quality. This could be attributed to two causes. Firstly, during evaporation, the liquid refrigerant boiled and turned to vapour, which has a higher specific volume than liquid. This led to an increase in the velocity of the two-phase flow, which resulted in the increasing heat transfer coefficient. Secondly, as the average quality increased, the liquid film thickness decreased, which decreased the thermal resistance in the liquid film and a higher heat transfer coefficient was obtained. These figures also show the effects of mass flux on the average heat transfer coefficient. It can be seen that the mass flux has a strong effect on the heat transfer performance, especially at high average quality. This effect may be explained by the previous studies by Berthoud and Jayanti [8] in that the interfacial vapour–liquid shear stress and the intensity of the secondary flow increased with increasing mass flux, which resulted in the enhancement of droplet entrainment and redeposition. This enhancement induced the increased number and larger size of waves on the liquid film surface, which increased the heat transfer area. In addition, the higher velocity, due to the increasing mass flux, increased the degree of turbulence of the fluid, which resulted in a higher heat transfer coefficient. However, the mass flux was found to have less effect on the heat transfer coefficient at low average quality. This may be because at low average quality, the two-phase flow velocity did not significantly increase with the mass flux as was found at high average quality.

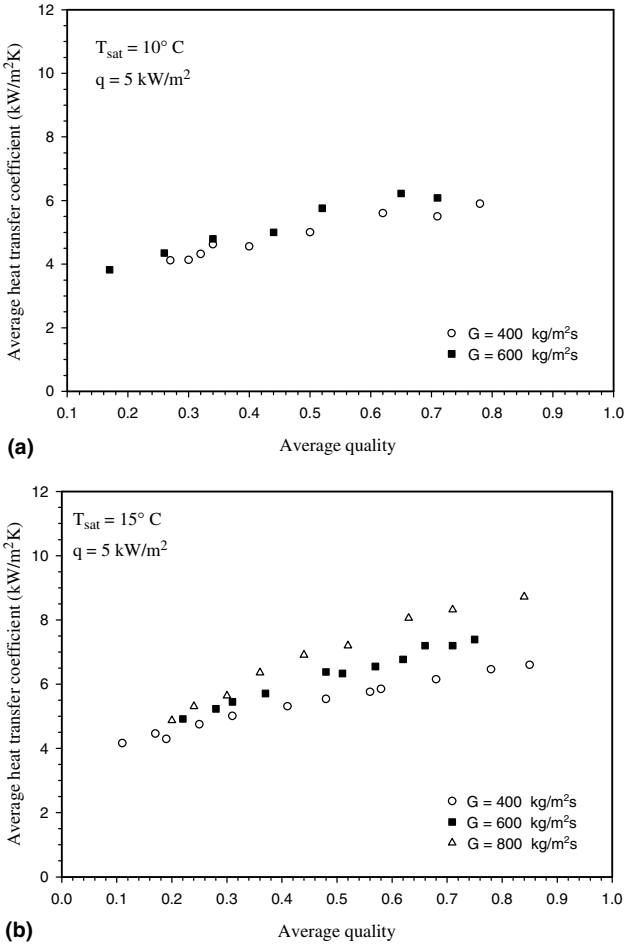

Fig. 3. Effect of mass flux on the average heat transfer coefficient.

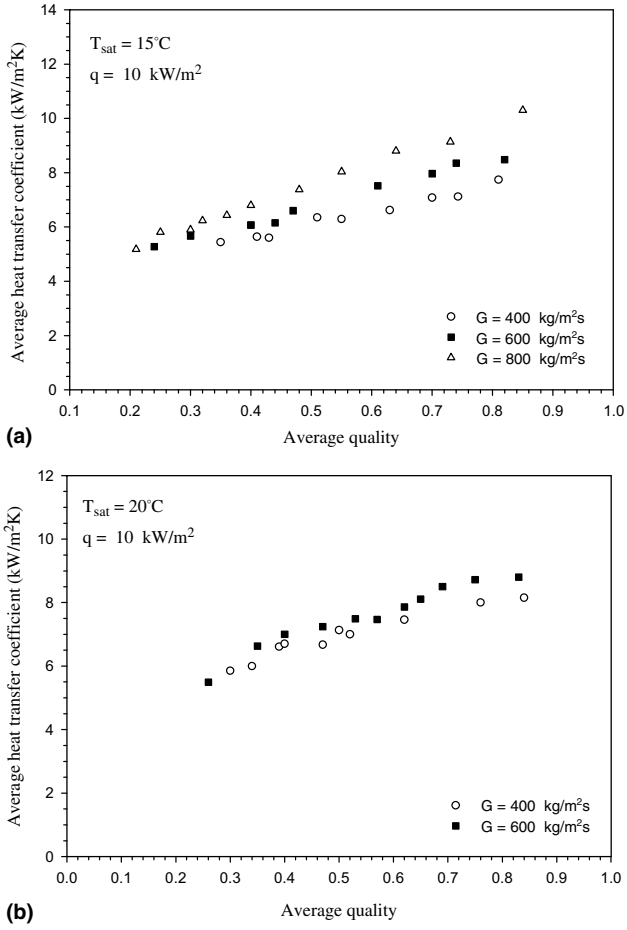

Fig. 4. Effect of mass flux on the average heat transfer coefficient.

4.1.2. Effect of temperature on average heat transfer coefficient

The effects of temperature on the average heat transfer coefficient at constant heat flux and mass flux, at various average qualities are illustrated in Figs. 5 and 6. The experimental data shows that the heat transfer coefficient tended to increase with increasing temperature. It was found that increasing temperature not only decreased the vapour specific volume and velocity [9] but also decreased the viscosity of the liquid film. As a result, the velocity of the liquid film increased and a higher degree of turbulence of liquid particles occurred.

4.1.3. Effect of heat flux on average heat transfer coefficient

Figs. 7 and 8 show variations of the average heat transfer coefficient with average quality at fixed mass flux, and saturation temperature. It is shown that the heat transfer coefficient increased with increasing heat flux. This can be explained in that the increase in heat flux increased the number of active nucleation sites, which increased the number of bubbles [10]. These bubbles have the significant effects on the flow behaviour as follow: induction of turbulent flow in the liquid film, acceleration of the two-phase velocity, and increase of the droplet entrainment. On the other hand, the increase in the number of bubbles resulted in the increase of the entrainment of droplets and the degree of turbulence, which resulted in a higher heat transfer coefficient.

4.1.4. Comparison of the present study with previous studies

The comparisons of the experimental results of the present study to those of previous studies are shown in Fig. 9. The results of this study, obtained from the tests on the helically coiled concentric tube-in-tube heat exchanger, were compared to those of Wongsa-ngam et al. [11], which were conducted on a straight concentric tube-in-tube heat exchanger. It was found that the helically coiled concentric tube-in-tube heat exchanger shows a 30–37% higher heat transfer performance than the straight concentric tube-in-tube heat exchanger. This can be explained in that the flow in the helically coiled concentric tube-in-tube heat exchanger was a different phase and more complicated than that in the straight concentric tube-in-tube heat exchanger due to the centrifugal force on liquid particles. This force induced secondary flow in the main stream of the two-phase flow. The liquid phase flowed along the circumferential

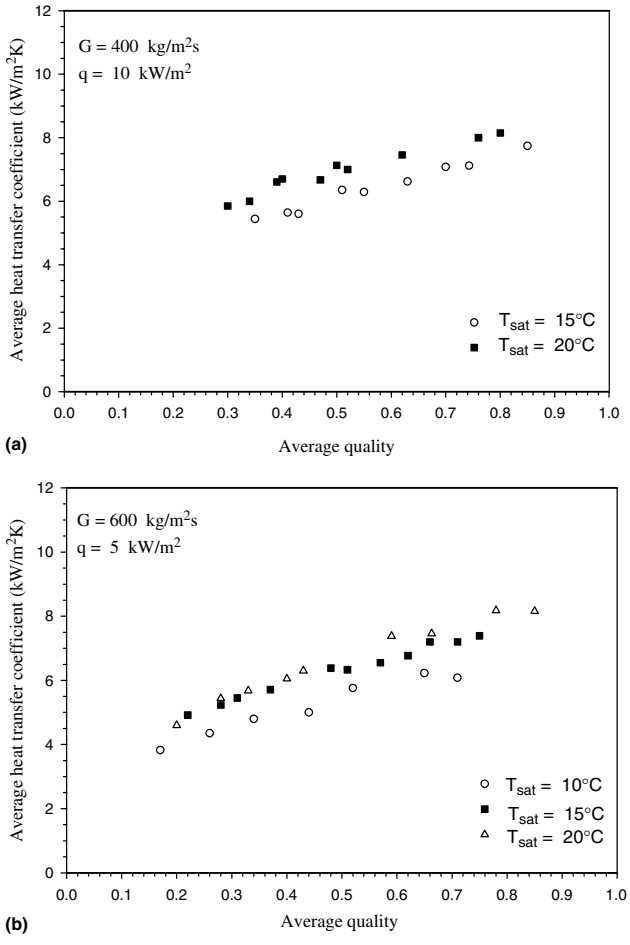

Fig. 5. Effect of temperature on the average heat transfer coefficient.

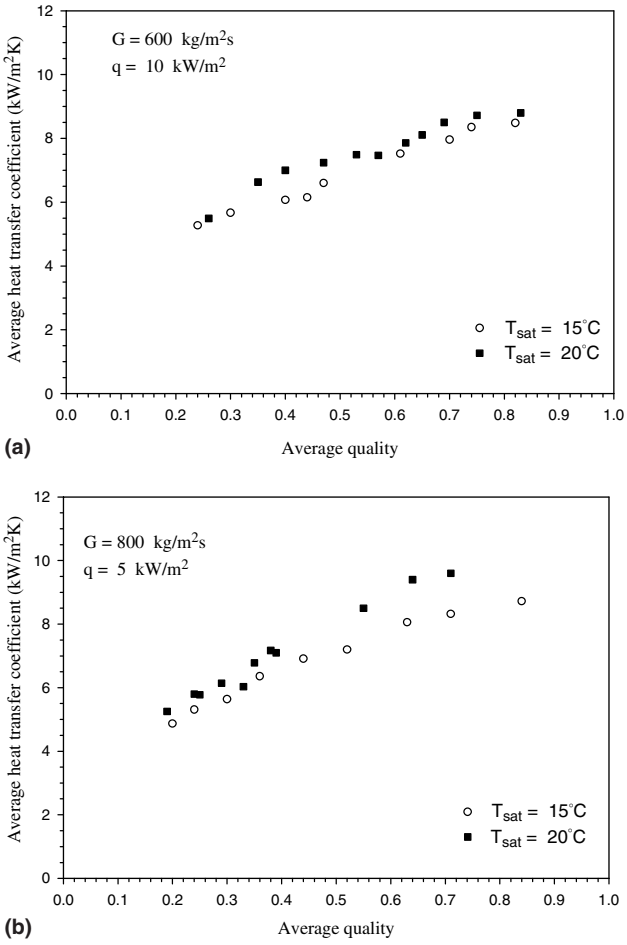

Fig. 6. Effect of temperature on the average heat transfer coefficient.

surface of the tube while the higher velocity vapour phase flowed at the core. As a result of the curvature influence, the vapour phase with higher velocity flowed in the form of a double vortex; outwards across the diameter of the tube and towards the centre of the curvature along the tube wall [12]. The secondary flow may have enhanced the heat transfer performance by the following mechanism:

- The velocity of fluid particles in the curved tube was higher than in the straight tube. This may be because the particles moved in a vortex making the particle move over a longer distance.
- The rate of entrainment and redeposition of droplets in the curved tube was found to be higher than in the straight tube. This phenomenon was induced by the secondary flow and increased the heat transfer area.

The heat transfer coefficient of refrigerant flowing in the helically coiled concentric tube-in-tube heat exchanger was therefore higher than that of the straight concentric tube-in-tube heat exchanger. In addition, when the average quality at which the partial dryout occurs in the helically coiled concentric tube-in-tube heat exchanger was compared to that in the straight concentric tube-in-tube heat exchanger, it was noted that the partial dryout in the helically coiled concentric tube-in-tube heat exchanger occurred at a higher average quality.

4.1.5. Evaporative heat transfer coefficient correlation for two-phase flow in helically coiled concentric tube-in-tube heat exchanger

There have been many studies in the past investigating the heat transfer performance of fluid flow in straight tubes. Hence, a number of empirical relations for predicting the heat transfer coefficient in this tube were proposed. However, there have been very few correlations for predicting the two-phase flow heat transfer coefficient in curved tubes. In this study, the correlation proposed by Jung et al. [13] and Cavallini and Zecchin [14] was modified for predicting the average heat transfer coefficient of HFC-134a during the evaporation in the helically coiled concentric tube-in-tube heat exchanger. The correlation expressed as a function of the boiling number, Bo; Martinelli parameter, χ_{tt}; equivalent Dean number, De_{Eq}; and Prandtl number, Pr as follows:

$$Nu_{\mathrm{tp}} = 6895.98 De_{\mathrm{Eq}}^{0.432} Pr_{\mathrm{l}}^{-5.055} (Bo \times 10^4)^{0.132} \chi_{tt}^{-0.0238} \quad (9)$$

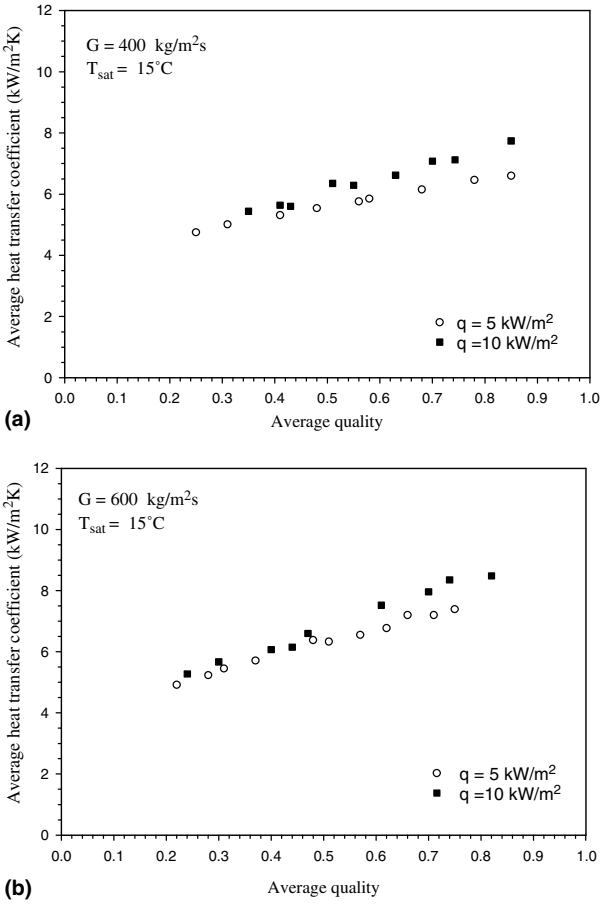

Fig. 7. Effect of heat flux on the average heat transfer coefficient.

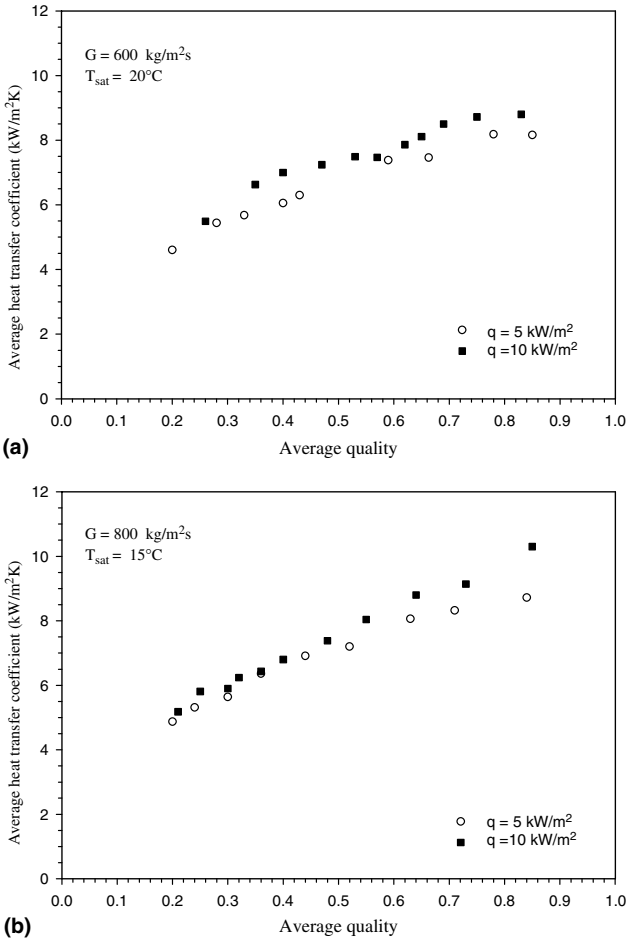

Fig. 8. Effect of heat flux on the average heat transfer coefficient.

Equivalent Dean number, De_{Eq}, is defined as

$$De_{Eq} = \left[Re_l + Re_v\left(\frac{\mu_v}{\mu_l}\right)\left(\frac{\rho_l}{\rho_v}\right)^{0.5}\right]\left(\frac{d_i}{D_c}\right)^{0.5} \quad (10)$$

Liquid Reynolds number, Re_l, is defined as

$$Re_l = \frac{G(1-x)d_i}{\mu_l} \quad (11)$$

Vapour Reynolds number, Re_v, is defined as

$$Re_v = \frac{Gxd_i}{\mu_v} \quad (12)$$

Prandtl number, Pr_l, is defined as

$$Pr_l = \frac{Cp_l\mu_l}{k_l} \quad (13)$$

Martinelli parameter, χ_{tt}, is defined as

$$\chi_{tt} = \left(\frac{1-x}{x}\right)^{0.9}\left(\frac{\rho_v}{\rho_l}\right)^{0.5}\left(\frac{\mu_l}{\mu_v}\right)^{0.1} \quad (14)$$

and boiling number, Bo, is defined as

$$Bo = \frac{q}{G.i_{lv}} \quad (15)$$

Fig. 10 shows the experimental heat transfer coefficient for HFC-134a as compared to the predicted values by the modified correlation. It can be seen that the experimental results agreed well with those predicted by the correlation, with a deviation of ±10%.

4.2. Pressure drop

The frictional pressure drop can be obtained by substracting the gravitational and accelerational terms from the experimental total pressure drop.

4.2.1. Effect of mass flux on pressure drop

Fig. 11 presents the frictional pressure drop during evaporation versus average quality with fixed saturation temperature and heat flux and at various mass fluxes. It was found that the pressure drop increased with increasing average quality for all mass fluxes. This may be because at higher average quality, vapour phase flows at higher velocity and affects the flow behaviour by enhancing the intensity of secondary flow. The droplet entrainment and redeposition increased due to the higher intensity of the secondary flow [8]. As a result, the liquid film flowed with a higher degree of turbulence and a higher interfacial

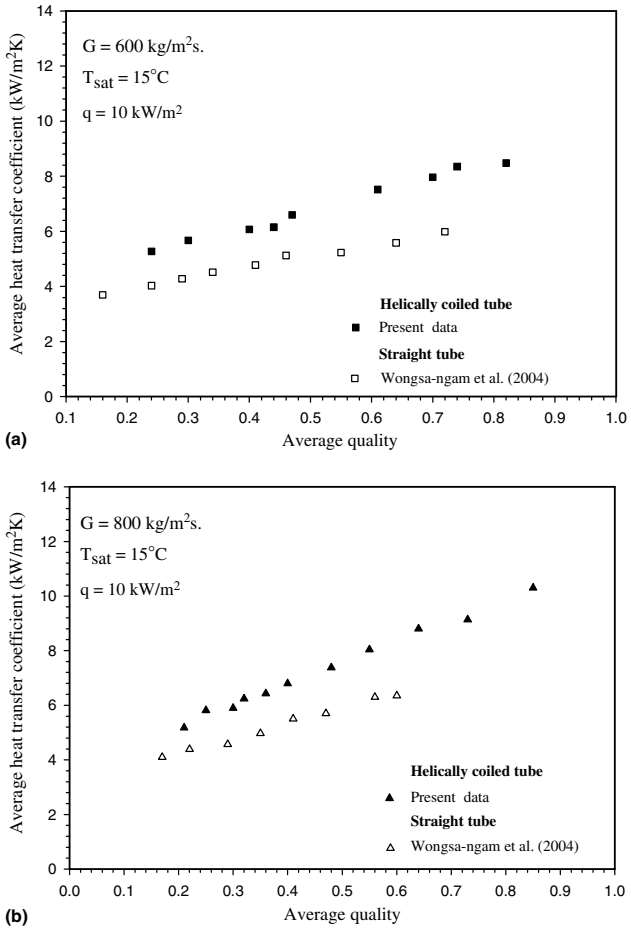

Fig. 9. Comparison of the average heat transfer coefficients.

vapour–liquid shear stress was established resulting in the higher-pressure drop.

At the same average quality, it was evident that the pressure drop increased with increasing mass flux. This can be explained in that the increase in mass flux accelerated the two-phase velocity, which led to higher intensity of secondary flow. Also, the numbers droplet entrainment and redeposition were increased due to secondary effects. Again, the higher velocity and interfacial vapour–liquid shear stress were presented. The pressure drop therefore increased with the mass flux.

4.2.2. Effect of saturation temperature on pressure drop

The variation of frictional pressure drop versus average quality at constant heat flux and mass flux are presented in Fig. 12. It can be seen that the increase in saturation temperature resulted in a decrease in the pressure drop. This may be attributed to the decrease in liquid viscosity and specific volume of the vapour, which decreased the vapour velocity and the shear stress between the interfacial vapour and liquid. As a result, a decrease in pressure drop was seen when the saturation temperature increased.

4.2.3. Effect of heat flux on pressure drop

Fig. 13 shows the variation of frictional pressure drop with average quality at constant mass flux and saturation temperature. The pressure drop tended to increase with increasing heat flux. The number of active nucleation sites increased as the heat flux increased, which resulted in a higher rate of bubble generation [10]. These bubbles agitated the liquid film and led to the increase in the turbulence in the liquid film. Moreover, the bubbles broke out at the liquid film surface and induced the entrainment and redeposition

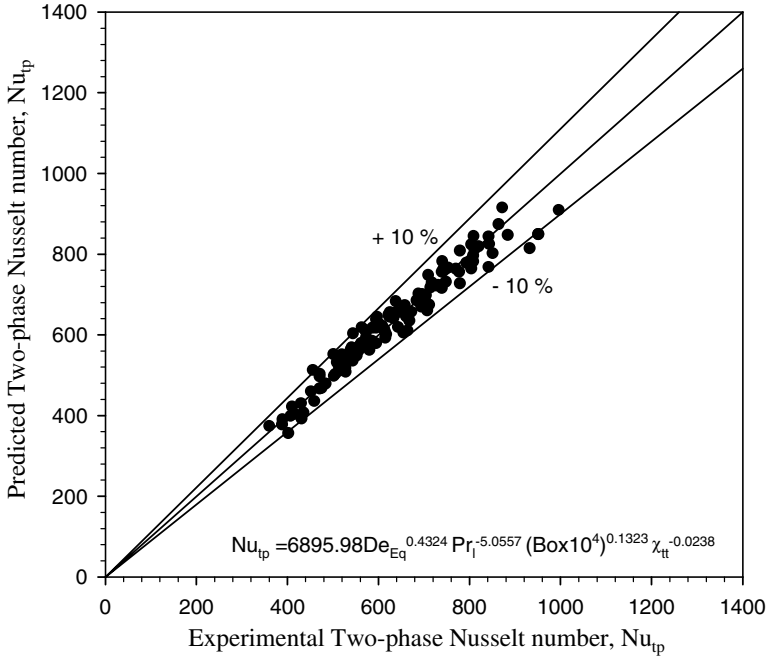

Fig. 10. Predicted Nusselt number using the proposed correlation versus the experimental Nusselt number.

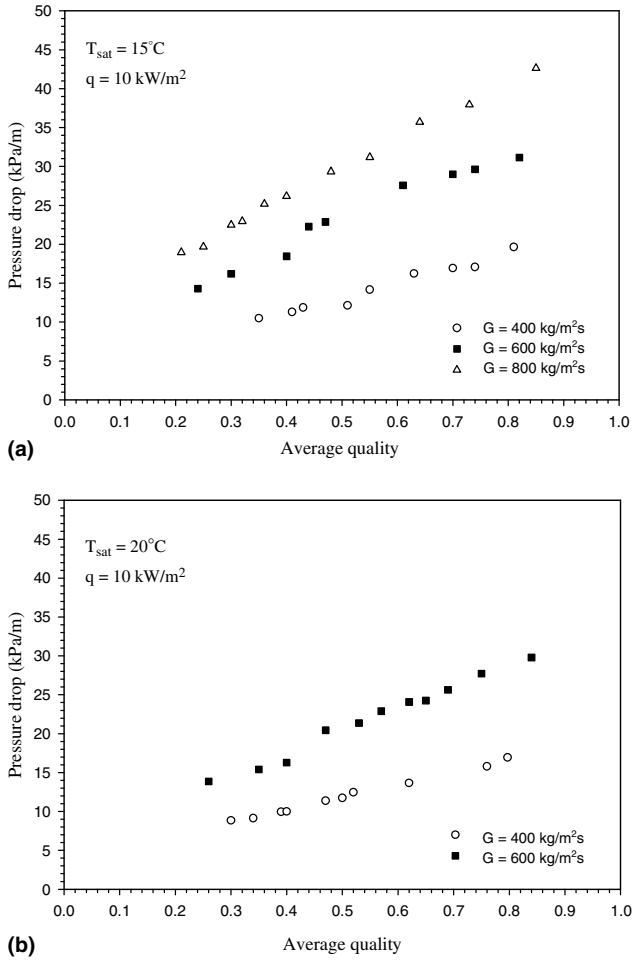

Fig. 11. Effect of mass flux on the pressure drop.

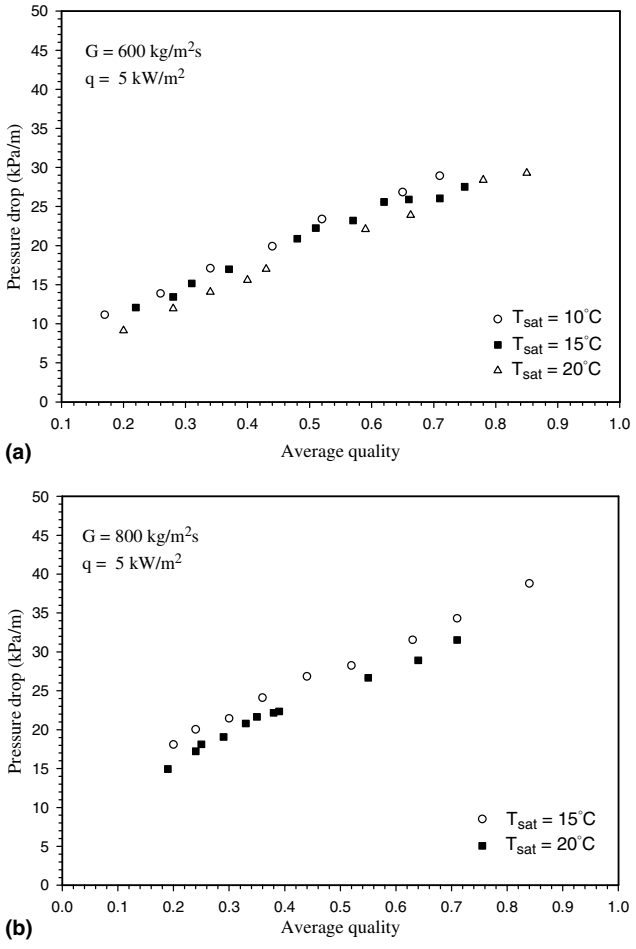

Fig. 12. Effect of temperature on the pressure drop.

of droplets. The disturbance by the droplet entrainment and redeposition not only induced the waves on the liquid film surface but also increased the shear stress. In addition, the higher rate of bubble generation due to the increase in active nucleation sites, accelerated the vapour velocity. The pressure drop then increased with the heat flux.

4.2.4. Frictional pressure drop correlations

In the gas–liquid two-phase flow, the frictional pressure gradient is correlated by the relationship between the two-phase frictional multiplier, ϕ_l^2, and parameter, χ [15] which can be obtained from the frictional pressure gradients of two-phase, liquid and gas flow components as follow:

$$\phi_l^2 = \left(\frac{dP_F}{dz}\right)_{tp} \Big/ \left(\frac{dP_F}{dz}\right)_l \tag{16}$$

The two-phase frictional pressure gradient, $\left(\frac{dP_F}{dz}\right)_{tp}$ can be obtained by substracting the gravitational and accelerational terms from the total experimental pressure gradient.

The single-phase liquid pressure gradient, $\left(\frac{dP_F}{dz}\right)_l$ can be calculated from

$$\left(\frac{dP_F}{dz}\right)_l = \frac{2f_l\rho_l U_l^2}{d_i} \tag{17}$$

where

$$f_l\left(\frac{D_c}{d_i}\right)^{0.5} = 0.00725 + 0.076\left[Re_l\left(\frac{D_c}{d_i}\right)^{-2}\right]^{-0.25} \tag{18}$$

It is noted that Eq. (18) was proposed by Ito [16] for calculating the fanning friction factor of fluid flowing in a curved tube.

The Martinelli parameter, χ^2 is given by

$$\chi^2 = \left(\frac{dP_F}{dz}\right)_l \Big/ \left(\frac{dP_F}{dz}\right)_v \tag{19}$$

If the two pressure gradients are based on turbulent flow

$$\chi = \chi_{tt} \approx \left(\frac{1-x}{x}\right)^{0.9}\left(\frac{\rho_v}{\rho_l}\right)^{0.5}\left(\frac{\mu_l}{\mu_v}\right)^{0.1} \tag{20}$$

The two-phase frictional multiplier for smooth circular tube can be proposed in form of Lockhart–Martinelli correlation as follows:

$$\phi_l^2 = 1 + \frac{C}{\chi_{tt}} + \frac{1}{\chi_{tt}^2} \tag{21}$$

The constant C in the equation is the parameter, which indicates the two-phase flow condition. The value of this parameter proposed by Chisholm [17] varying from 5 to

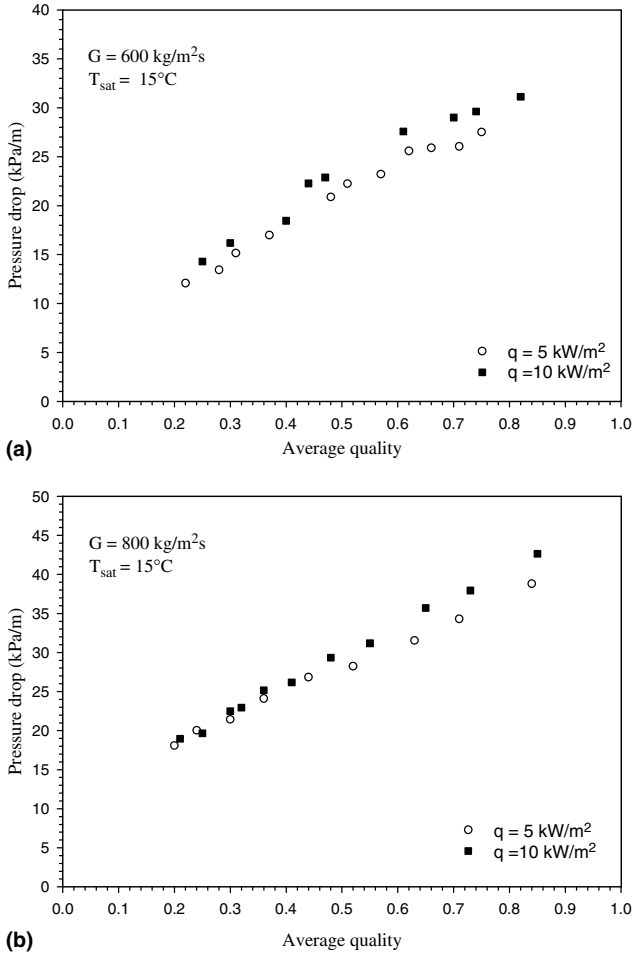

Fig. 13. Effect of heat flux on the pressure drop.

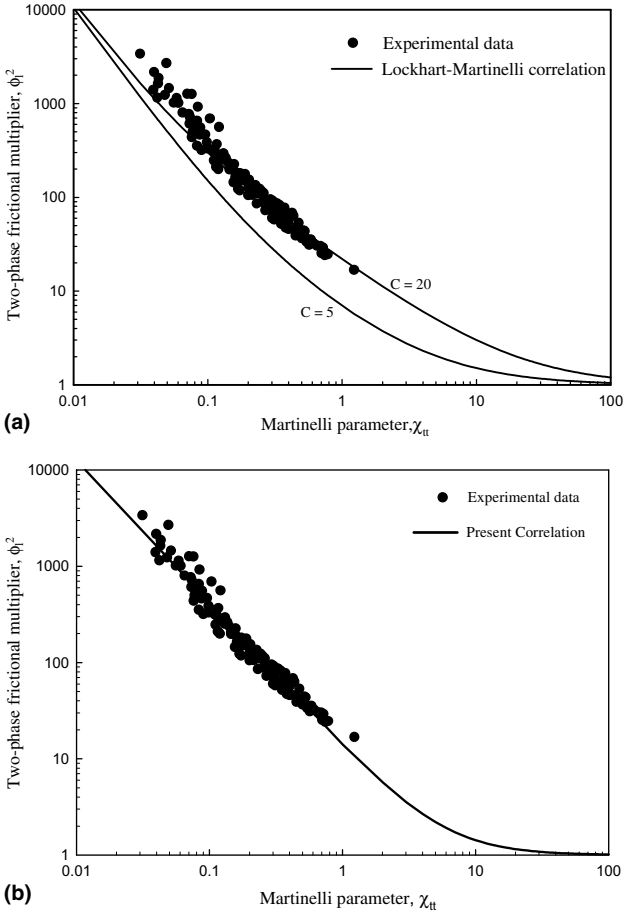

Fig. 14. Martinelli parameter versus the two-phase frictional multiplier.

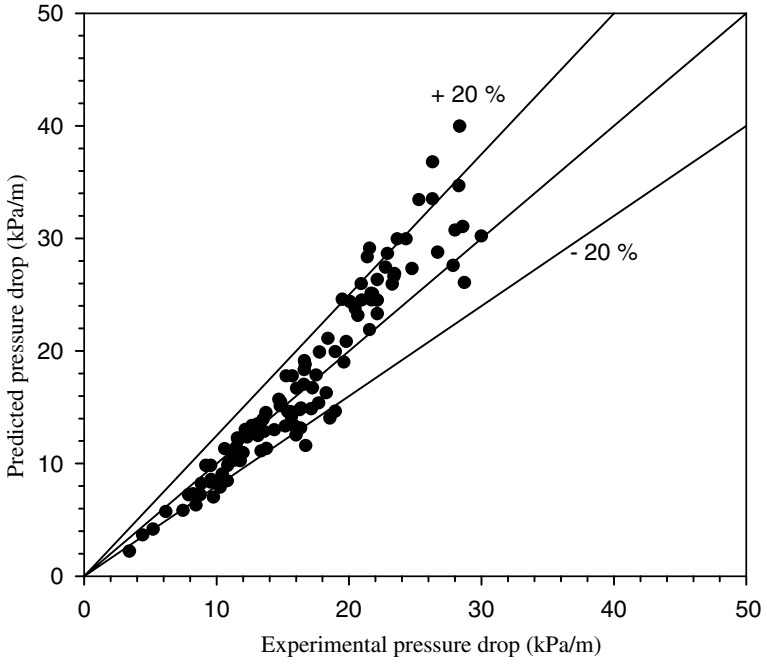

Fig. 15. Predicted pressure drop versus the measured pressure drop.

20, depends on the flow condition of the vapour and liquid. For instance, the constant $C = 20$ when the vapour and liquid flow in the turbulent region, and $C = 5$ if the two-phase flow is in the laminar region. Comparison of experimental frictional pressure gradient with the Lockhart–Martinelli correlation is shown in Fig. 14(a). The correlation with $C = 5$ and 20 are shown by a solid line in the figure. It was found that the two-phase flow in the helically coiled concentric tube-in-tube heat exchanger had a very high degree of turbulence.

A new correlation for predicting the two-phase frictional multiplier was proposed. This correlation was modified from the correlation proposed by Soliman et al. [18], which was simple and predicted accurately. The proposed correlation used in calculating the two-phase flow frictional multiplier is $\phi_1^2 = 1 + C/\chi_{tt}^m$. The experimental results of this study were used in calculating the parameter in the correlation of Soliman by means of regression. The new correlation for calculating the two-phase frictional multiplier was then obtained as follows:

$$\phi_1^2 = 1 + \frac{13.37}{\chi_{tt}^{1.492}} \tag{22}$$

The ϕ_1^2, which was determined by using Eq. (22) is shown in Fig. 14(b) as a black solid line. In order to predict the frictional pressure gradient, the calculation result from Eq. (22) is inserted in Eq. (16). Fig. 15 shows experimental frictional pressure gradient plotted against predicted frictional pressure gradient obtained from Eq. (22). It is clear from this figure that the majority of the data falls within ±20% of the proposed correlation.

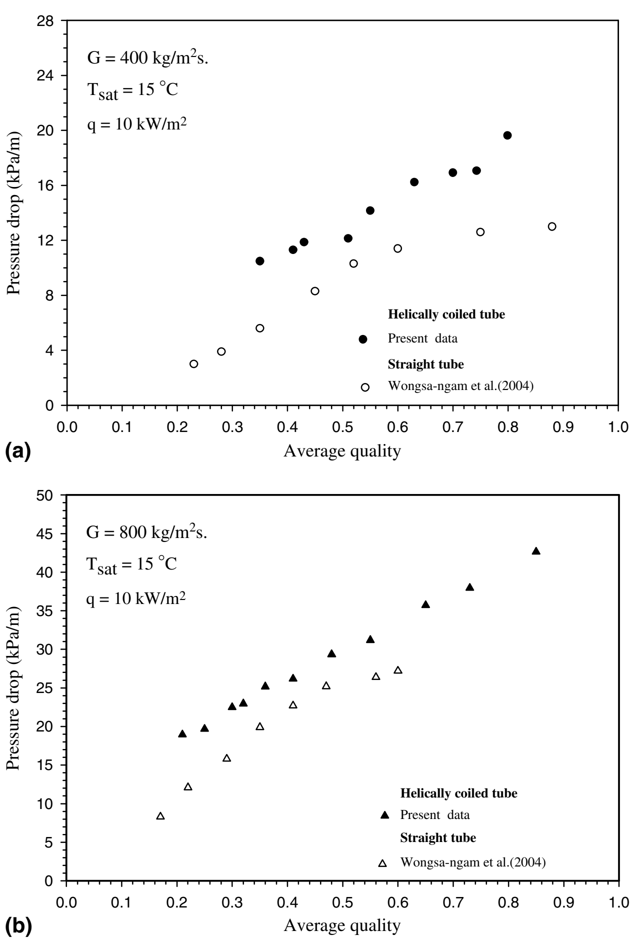
(a)
G = 400 kg/m²s.
Tsat = 15 °C
q = 10 kW/m²
Pressure drop (kPa/m)
Average quality
Helically coiled tube
Present data
Straight tube
Wongsa-ngam et al.(2004)
(b)
G = 800 kg/m²s.
Tsat = 15 °C
q = 10 kW/m²
Pressure drop (kPa/m)
Average quality
Helically coiled tube
Present data
Straight tube
Wongsa-ngam et al.(2004)

Fig. 16. Comparison of the pressure drop.

4.2.5. *Comparison of the result from the present study with those of the previous study*

The results of this study were compared to those conducted by Wongsa-ngam et al. [11] at the same experimental conditions, as shown in Fig. 16. The pressure drop in the helically coiled concentric tube-in-tube heat exchanger was found to be higher than in the straight concentric tube-in-tube heat exchanger by 10–73%. This may be because of the differences in the flow characteristics of two-phase fluid flowing in straight and curved tubes, as described in the previous sections.

5. Conclusions

This study was conducted to investigate the average heat transfer coefficient and pressure drop during evaporation of refrigerant HFC-134a at high mass flux. In the test, the refrigerant was maintained in two-phase condition during flow in the test section and the data was recorded when the system was in steady state. The experimental results were processed and the conclusions are as follow:

1. The average heat transfer coefficient of HFC-134a during evaporation tended to increase with increasing average quality, mass flux, heat flux and saturation temperature.
2. The pressure drop in the test section increased with increasing average quality, mass flux and heat flux but tended to decrease with increasing saturation temperature.
3. The average heat transfer coefficient of HFC-134a flowing in helically coiled concentric tube-in-tube heat exchanger was higher than in straight concentric tube-in-tube heat exchanger by 30–37%. The frictional pressure drop presented in these heat exchangers was found to be higher than in straight concentric tube-in-tube heat exchangers by 10–73%. The partial dryout in concentric spiral double-tube heat exchangers was found at a higher average quality than in straight concentric tube-in-tube heat exchangers.
4. The correlation for predicting the average heat transfer coefficient and pressure drop during evaporation can be expressed as follows:
   4.1. Average heat transfer coefficient:
   $$Nu_{\text{tp}} = 6895.98 De_{\text{Eq}}^{0.432} Pr_1^{-5.055} (Bo \times 10^4)^{0.132} \chi_{tt}^{-0.0238}$$
   4.2. Two-phase frictional multiplier correlation, as used in calculating frictional pressure drop:
   $$\phi_1^2 = 1 + \frac{13.37}{\chi_{tt}^{1.492}}$$

Acknowledgement

The present study was financially supported by the Thailand Research Fund (TRF) whose guidance and assistance are gratefully acknowledged.

References

[1] S. Garimella, D.E. Richards, R.N. Christensen, Experimental investigation of heat transfer in coiled annular duct, Trans. ASME 110 (1988) 329–336.
[2] R.C. Xin, A. Awwad, Z.F. Dong, M.A. Ebadian, An experimental study of single-phase and two-phase flow pressure drop in annular helicoidal pipes, Int. J. Heat Mass Transfer 18 (1997) 482–488.
[3] H.J. Kang, C.X. Lin, M.A. Ebadian, Condensation of R-134a flowing inside helicoidal pipe, Int. J. Heat Mass Transfer 43 (2000) 2553–2564.
[4] T.J. Rennie, G.S.V. Raghavan, Laminar parallel flow in a tube-in-tube helical heat exchanger,the AIC 2002 Meeting CSAE/SCGR Program Saskatoon, Saskachewan, Paper No. 02-406, 2002.
[5] B. Yu, J.R. Han, H.J. Kang, C.X. Lin, A. Awwad, M.A. Ebadian, Condensation heat transfer of R-134a flow inside helical pipes at different orientations, Int. Commun. Heat Mass Transfer 30 (2003) 745–754.
[6] W.I. Louw, J.P. Meyer, Annular tube contact in a helically coiled tube-in-tube heat exchanger, in: Proceedings of the second International Conference on Heat Transfer, Fluid Mechanics and Thermodynamics, Victoria Falls, Zambia, 23–26 June, 2003.
[7] M.O. McLinden, S.A. Klein, E.W. Lemmon, REPROP, Thermodynamic and transport properties of refrigerants and refrigerant mixtures. NIST Standard Reference Database—version 6.01, 1998.
[8] G. Berthoud, S. Jayanti, Characterization of dryout in helical coils, Int. J. Heat Mass Transfer 33 (1990) 1451–1463.
[9] K. Seo, Y. Kim, Evaporation heat transfer and pressure drop of R-22 in 7 and 9.52 mm smooth/micro-fin tube, Int. J. Heat Transfer 43 (2000) 2869–2882.
[10] C.B. Chiou, D.C. Lu, C.C. Wang, Pool boiling of R-22, R-124 and R-134a on a plain tube, Int. J. Heat Mass Transfer 40 (1996) 1657–1666.
[11] J. Wongsa-ngam, T. Nualboonrueng, S. Wongwises, Performance of smooth and micro-fin tubes in high mass flux region of R-134a during evaporation, Heat Mass Transfer 10 (2002) 425–435.
[12] A. Owhadi, J.B. Kenneth, B. Crain, Forced convection boiling inside helically-coiled tubes, Int. J. Heat Mass Transfer 11 (1968) 1779–1793.
[13] D. Jung, K.H. Song, Y. Cho, S. Kim, Flow condensation heat transfer coefficients of pure refrigrants, Int. J. Refrig. 26 (2003) 4–11.
[14] A. Cavallini, R. Zecchin, A dimensionless correlation for heat transfer coefficient in forced convection condensation, in: Proceedings of the Sixth International Heat Transfer Conference, Tokyo, 1974, pp. 309–313.
[15] R.W. Lockhart, R.C. Martinelli, Proposed correlation of data for isothermal two-phase two-component flow in pipes, Chem. Eng. Progress 45 (1949) 39–48.
[16] H. Ito, Frictional factor for turbulent flow in curved pipes, Trans. ASME, J. Basic Eng. 81 (1959) 123–134.
[17] D. Chisholm, A theoretical basis for the Lockhart–Martinelli correlation for two-phase flow, Int. J. Heat Mass Transfer 10 (1967) 1767–1778.
[18] M. Soliman, J.R. Schuster, P.J. Berenson, A general heat transfer correlation for annular flow condensation, J. Heat Transfer (1968) 267–276.